Science
Reprint

Cooperation Between Translating Ribosomes and RNA Polymerase in Transcription Elongation

Sergey Proshkin, A. Rachid Rahmouni, Alexander Mironov, Evgeny Nudler

23 April 2010
Volume 328, pp.504-508

Cooperation Between Translating Ribosomes and RNA Polymerase in Transcription Elongation

Sergey Proshkin,[1,2] A. Rachid Rahmouni,[3] Alexander Mironov,[2] Evgeny Nudler[1]*

During transcription of protein-coding genes, bacterial RNA polymerase (RNAP) is closely followed by a ribosome that translates the newly synthesized transcript. Our in vivo measurements show that the overall elongation rate of transcription is tightly controlled by the rate of translation. Acceleration and deceleration of a ribosome result in corresponding changes in the speed of RNAP. Moreover, we found an inverse correlation between the number of rare codons in a gene, which delay ribosome progression, and the rate of transcription. The stimulating effect of a ribosome on RNAP is achieved by preventing its spontaneous backtracking, which enhances the pace and also facilitates readthrough of roadblocks in vivo. Such a cooperative mechanism ensures that the transcriptional yield is always adjusted to translational needs at different genes and under various growth conditions.

In contrast to eukaryotes, where translation and transcription take place in different cellular compartments, in bacteria, the two principal events of gene expression are coupled in time and space. The majority of bacterial genes initiate translation soon after the ribosome-binding site (RBS) has emerged from the RNA exit channel of RNA polymerase (RNAP). Although translation-transcription coupling has been known for decades, its function was ascribed only in specific cases of transcription attenuation and polarity (*1*). When a ribosome slows down owing to, for example, amino acid deficiency, the growing gap between moving RNAP and lagging ribosome provides the termination factor Rho with access to the nascent RNA, which results in premature termination of downstream genes—a phenomenon known as the polarity effect (*2*). The ribosome can also be responsible for early transcription termination at certain metabolic operons, by allowing the formation of an intrinsic termination hairpin in the leader RNA sequences that leads to transcription attenuation (*3*). Notably, both attenuation and polarity occur when the ribosome and

[1]Department of Biochemistry, New York University School of Medicine, New York, NY 10016, USA. [2]State Research Institute of Genetics and Selection of Industrial Microorganisms, Moscow 117545, Russia. [3]Centre de Biophysique Moléculaire, CNRS, Rue Charles Sadron, 45071 Orléans, France.

*To whom correspondence should be addressed. E-mail: evgeny.nudler@nyumc.org

RNAP are physically separated. In each case, the effect of a ribosome on RNAP is indirect; it is mediated by either Rho factor or RNA secondary structures. In contrast, we found that for most of the coding region, the first trailing ribosome directly assists RNAP during elongation. Such cooperation between the two macromolecules explains the precise match of translational and transcriptional rates under various growth conditions (Table 1).

To measure the overall transcription elongation rate in vivo, we used a plasmid carrying the isopropyl-β-D-thiogalactopyranoside (IPTG)–inducible version of the A1 promoter of bacteriophage T7 fused to the *lacZ* reporter gene (*4*) (Fig. 1A). To calculate the elongation rate, the *Escherichia coli* culture was induced with IPTG, and the time that elapsed between the appearance of a specific hybridization signal from probes complementary to the 5′ and 3′ segments of the *lacZ* transcript was determined by dot-blot hybridization (Fig. 1 and fig. S1) (*5*, *6*). Although the absolute values of the hybridization signal may vary depending on factors such as Rho termination, RNA stability, or rate of transcription initiation, the timing for the linear signal increase between the two probes depends only on RNAP speed. This setup therefore allows an accurate and unbiased determination of the elongation rate in vivo (*5*, *6*). In parallel, we measured the translation elongation rate by monitoring the induction lag for β-galactosidase synthesis (fig. S2) (*7*). We first investigated the effect of the antibiotic chloramphenicol (Cm), a specific inhibitor of translation elongation, on the transcription elongation rate. Cm was added to exponentially growing cells at 1 μg/ml, a concentration that had only a mild inhibitory effect on bacterial growth. In the absence of Cm, the transcription elongation rate was determined to be 42 nucleotides (nt) per second under specified growth conditions, matching a translation elongation rate of 14 amino acids per second (Table 1 and fig. S2). However, Cm reduced the transcription elongation rate to 27 nt/s (Fig. 1B), which matched a reduced translation rate of nine amino acids per s (Table 1 and fig. S2). This result suggests that the ribosome controls the rate of RNAP propagation.

To provide further support for this conclusion and to rule out any potential indirect effect of Cm on transcription, we took advantage of a bacterial strain carrying a chromosomal mutation in the *rpsL* gene that renders the ribosome inherently slow (*4*, *8*). It is advantageous that the slow translation phenotype of this mutant (CH184 cells) can be partially recovered by the antibiotic streptomycin (Sm), which also restores the growth rate of the mutant strain (*8*). Indeed, our β-galactosidase measurements indicate that, without Sm, the translation elongation rate of CH184 was 6 amino acids per s and, in the presence of 100 μg/ml Sm, 10 amino acids per s (Table 1 and fig. S2), results that are consistent with a previous study (*8*). The speed of transcription elongation in CH184 was remarkably slow (only 19 nt/s), but accelerated to 30 nt/s when Sm was added (Fig. 1C), which perfectly matched the translation elongation rates with and without Sm (Table 1). The opposite effect of translation antibiotics (Cm and Sm) on transcription elongation demonstrates a strong reliance of RNAP speed on that of a ribosome.

Codon usage affects the rate of translation in bacteria and other organisms (*9*–*11*). Rare codons, which pair to less-abundant transfer RNA isoacceptors, delay the progression of a ribosome and often compromise protein expression (*12*–*14*). If the transcriptional rate relies so heavily on translation, the codon-reading program encoded by each individual gene should determine the speed of RNAP. To test this hypothesis, we compared the rates of transcription elongation at several genes with different rare codon frequency (*4*). The *E. coli* genes *rplB* and *tufA* have a relatively small number of rare codons (Table 2 and fig. S3). In contrast, a foreign gene (*srb4*) that encodes a subunit of the yeast Mediator is characterized by a high frequency of rare codons (Table 2 and fig. S3). Open reading frames of the *rplB-tufA* fusion and *srb4*, which are the same length (2 kb), were inserted upstream of *lacZ* in the same test vector used in our previous experiments (Fig. 1D). Remarkably, transcription of *rplB-tufA* matched its fast translation rate and was more than 1.5 times as fast as that of *srb4* (Fig. 1D and Table 2). Moreover, genes carrying an intermediate number of rare codons (*lacZ* and *infB*) predictably displayed intermediate rates of transcription (Table 2). Thus, codon usage is a key determinant of transcription rate.

Previously, we showed that the rate of transcription elongation depends on the efficiency of initiation as determined by promoter strength (*5*, *15*). The mechanism underlying this phenomenon was explained by the cumulative anti-backtracking effect of trailing elongation complexes (ECs) on the leading EC (fig. S4). Backtracking or spontaneous reverse sliding of the EC along DNA and RNA occurs frequently in vitro and usually determines the overall elongation rate (*5*, *15*). During backtracking, the 3′ end of RNA is disengaged from the RNAP catalytic site, which causes pausing or permanent EC inactivation (*16*, *17*). The leading backtracked ECs in vitro can be rescued by trailing ECs that push them forward (*5*, *15*). The trailing ribosome could similarly control the rate of transcription by "pushing" backtracked ECs forward (fig. S4).

To test this hypothesis, we developed an assay in which the effect of a ribosome on RNAP backtracking could be directly monitored in vivo (*4*). We constructed a set of plasmids in which RNAP initiated from a constitutive promoter is halted at a downstream site by the *lac* repressor bound to its operator motif (Fig. 2A). Previously, we showed that RNAP backtracks when it collides with the repressor in vitro and in vivo, which restricts its ability to readthrough the roadblock (*15*). To monitor the changes in positioning of the blocked EC in response to translation, we performed in situ footprinting of the transcription bubble with the single strand–specific probe, chloroacetaldehyde (CAA) (Fig. 2B) (*15*). The plasmids were designed so that the repressor halted either two ECs transcribing in tandem (p2EC) or only one isolated EC (p1EC) (Fig. 2). In the latter case, the trp terminator was placed between the promoter and the *lac* repressor-binding site to completely terminate the trailing EC upon stalling (*15*). A derivative of p1EC (p^{RBS}1EC) was also made, which contained the strong ribosome-binding site (RBS) derived from gene 10 of bacteriophage T7 positioned 120 nt upstream of the *lac* repressor-binding site (Fig. 2A). Analysis of CAA modifications on the nontemplate strand of p2EC and p1EC revealed two ECs (nos. 1 and 2) and one EC (no. 1) between the promoter and the repressor,

Table 1. Overall transcription elongation rates match that of translation under various growth conditions. MG1655 (wild type) and CH184 (*rpsL*[SmP]) were grown in Luria broth to the exponential phase ($OD_{600} \approx 0.4$) before IPTG induction, unless indicated otherwise. Stationary phase, IPTG was added at $OD_{600} \approx 2.5$. Alternative carbon sources: Glycerol, cells were grown in M9 minimal media supplemented with glycerol (0.5%) and casamino acids (0.2%); αMG, cells were grown in glucose minimal media in the presence of α-methyl-glucoside, at the 15:1 glucose ratio. IPTG was added at $OD_{600} \approx 0.4$. Numbers represent averaged values from three independent experiments ($P < 0.05$), including those described in Fig. 1 and figs. S2, S5, S6, and S7. The standard error for each value in each individual experiment was less than 10%.

Strain	Growth condition	Transcription rates (nt/s)	Translation rates (amino acids per s)	Ratio of nt to amino acid
MG1655		42	14	3.0
MG1655	+ Cm	27	9	3.0
MG1655	Stationary	21	7	3.0
MG1655	Glycerol	31	10	3.1
MG1655	αMG	23	8	2.9
CH184	+ Sm	31	10	3.1
CH184		19	6	3.2
CH184	Stationary + Sm	22	7	3.1
CH184	Stationary	12	4	3.0

respectively (Fig. 2B). CAA signals from ECs 1 and 2 disappeared when IPTG was added, which demonstrated that, in each case, the *lac* repressor blocked the ECs (*15*). CAA footprinting revealed a significant difference in positioning of EC1 on each plasmid. Clearly, isolated EC1 in p1EC backtracks over a longer distance than EC1 in p^{RBS}1EC (or in p2EC), because new CAA reactive sites are detected upstream and the reactivity of the downstream margin of the footprint is strongly decreased (Fig. 2B, compare lanes 2 and 3). We conclude that similarly to the situation with trailing ECs (lane 1) (*15*), the trailing ribosome prevents backtracking of the leading EC.

Because trailing ECs help leading ECs traverse the roadblock by inhibiting backtracking (*15*), the inhibition of backtracking by a ribosome should also facilitate transcriptional readthrough. This premise was tested directly by comparing the amounts of downstream *cat* mRNA generated from p^{RBS}1EC and p1EC plasmids, with and without the translation inhibitors spectinomycin (Sp) and tetracycline (Tc) (*4*) (Fig. 3A). *Cat* message accumulation was measured by reverse-transcriptase primer extension and normalized to the plasmid-encoded β-lactamase transcript (bla) (Fig. 3B). Without RBS, only ~10% of ECs were transcribed beyond the roadblock (lane 1). However, the level of readthrough increased to 40% for RBS-containing plasmid (lane 3). Moreover, the ribosome-targeting antibiotics reversed the stimulating effect of RBS on transcriptional readthrough (lane 5). Because the space between the blocked RNAP and RBS can accommodate only one ribosome at a time, this analysis revealed direct in vivo cooperation between a single moving ribosome and a single moving RNAP in overcoming the transcriptional roadblock.

RNAP and ribosomes are two molecular motors with fundamentally different working cycles. Although both enzymes use Brownian ratchet principles in converting thermal energy into movement (*18*–*20*), translocation of a ribosome is virtually irreversible, whereas RNAP oscillates back and forth along RNA and DNA at numerous sites in vitro (*16*, *17*, *20*, *21*). Such an equilibrium between productive and nonproductive (pretranslocated or backtracking) states determines the pace of transcription elongation (*20*). Elongation factors, such as NusG or RfaH, shift the equilibrium toward the productive (posttranslocated) state. They accelerate transcription by changing the intrinsic translocation properties of RNAP (*20*, *22*). In contrast, a moving ribosome appears to control transcription "mechanically," by physically blocking backtracking (Fig. 2 and fig. S4) (*23*). Such cooperation between RNAP and a ribosome is reminiscent of trailing ECs helping leading ECs to overcome backtracking-type elongation blocks in vitro and in vivo (*5*, *15*, *24*). The cooperation effect in this case

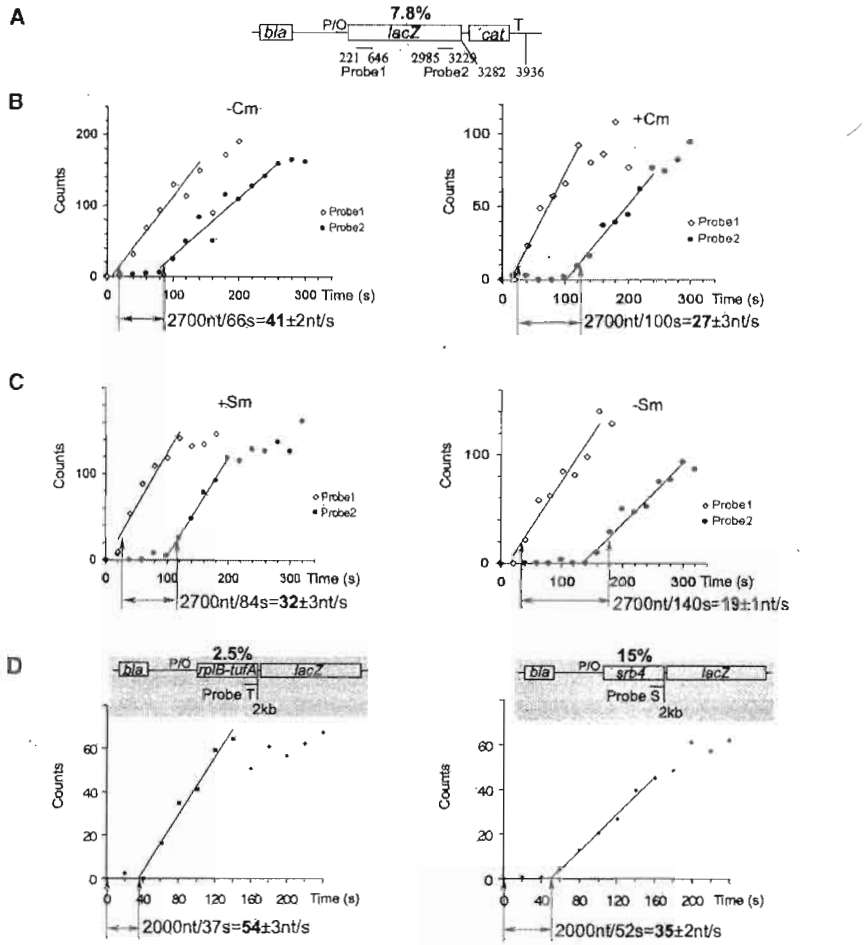

Fig. 1. The overall transcription elongation rate depends on the rate of translation. **(A)** Schematics of the test plasmid pUV12 used in (B) and (C) (*5*, *6*). White bars show genes. P/O indicates the $T7A1_{04/03}$ promoter-operator site; T, the terminator sequence. Lines indicate probes complementary to the *lacZ* transcript at specified positions relative to the 5′ end. The percentage of rare codons in the open reading frame (%) is indicated on top. **(B)** Effect of chloramphenicol (Cm) on transcription elongation rate. Panels display representative induction curves used to calculate the elongation rate. At time 0, IPTG was added. RNA was extracted at the indicated times after induction and used for parallel dot-blot hybridization with the early (probe 1) and late (probe 2) *lac* probes (fig. S1A). The distance between probes divided by the time of the linear increase in the hybridization signal between probes 1 and 2 (shown by arrows) gives the elongation rate. Radioactivity at time 0 (before IPTG induction) was taken as background and subtracted from all values. **(C)** Effect of the slow ribosome mutant (SmP) and streptomycin (Sm) on transcription elongation rate. Representative induction curves used to calculate the elongation rate. Corresponding dot blots of the early (probe 1) and late (probe 2) probes are shown in fig. S1B. **(D)** Rate of transcription elongation as a function of codon usage. Schematics of the test plasmids with the percentage of rare codons in the open reading frame (%) are shown on top. Two representative induction curves used to calculate the elongation rate are displayed. The amount of radioactivity in each probe was divided by the corresponding radioactivity in the *bla* probe, and the ratio is plotted against sampling time. Corresponding dot blots are shown in fig. S1C. The distance between the probe and the start of transcription divided by the time of linear increase in the hybridization signal (shown by arrows) gives the elongation rate.

Table 2. Inverse correlation between rare codon frequency and transcription elongation rates at individual genes. The percentage (%) of rare codons in each gene tested is indicated in parentheses. All numbers except those with asterisk(s) represent averaged values from three independent experiments ($P < 0.05$), including those described in Fig. 1 and fig. S2. ND, not determined.

Gene	Rare codons/length (%)	Translation rates (amino acids per s)	Transcription rates (nt/s)
rplB-tufA	16/639 (2.5)	18 ± 2*	54
infB	30/891 (3.3)	ND	45†
lacZ	80/1025 (7.8)	14	42
srb4	102/688 (15)	ND	35

*Value from (*29*). †Value from (*6*).

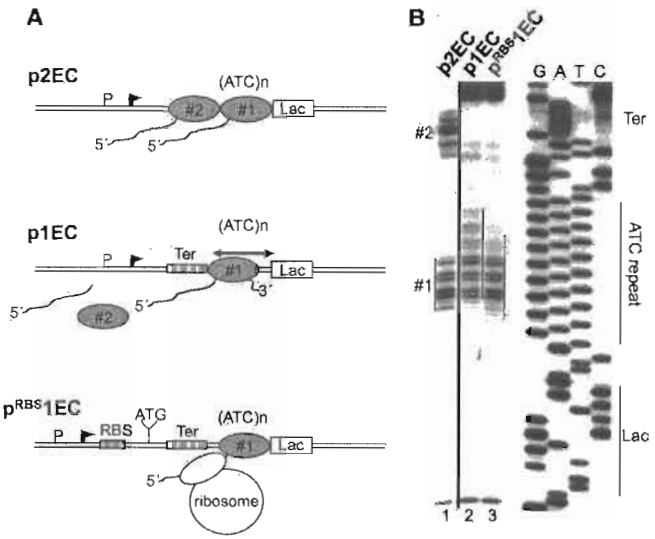

Fig. 2. The trailing ribosome inhibits RNAP backtracking. **(A)** Diagram describing p2EC, p1EC, and p^{RBS}1EC constructs and footprinting results of **(B)**. The leading EC1 is halted by the *lac* repressor within the ATC repeated sequence (ATC)*n*. The trpT terminator (Ter) is positioned so that the trailing EC (EC2) stalled at the termination site dissociates completely. **(B)** Primer extension analyses of in situ CAA modifications of the nontemplate strand in p2EC (line 1), p1EC (line 2), and p^{RBS}1EC (line 3). The locations of the lac operator (Lac), ATC repeat, terminator (Ter), EC1, and EC2 are indicated. Red lines show the dynamic position of the EC1 transcription bubble. The presence of EC2 or trailing ribosome shifts the backtracked EC1 forward. The space between the RBS and blocked EC1 allows for only one ribosome to be engaged in translation.

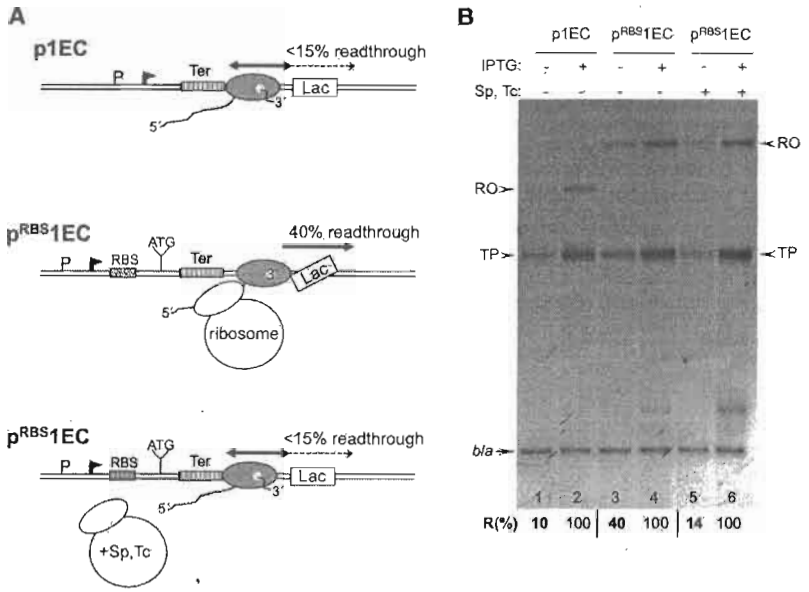

Fig. 3. Cooperation between the ribosome and leading RNAP in overcoming a transcriptional roadblock in vivo. **(A)** Diagram describing the cooperative mechanism and the results of (B). The ribosome reactivates the blocked EC (which is predominantly backtracked) by "pushing" it forward. The activated EC is now able to traverse the *lac* repressor, as soon as the latter dissociates. Inhibition of translation by antibiotics (Sp and Tc) disrupts cooperation, thereby inhibiting RNAP readthrough. **(B)** Stimulating effect of translation on transcriptional readthrough of the *lac* repressor in vivo. Autoradiogram shows the RT extension products obtained from ^{32}P primers hybridized to either *cat* or *bla* transcripts. p1EC and p^{RBS}1EC template plasmids and experimental conditions were as in Fig. 2. The ribosome inhibitors Sp and Tc were added as indicated (lanes 5 and 6). RO and TP stand for the full size (runoff) reverse transcription product and the product interrupted at the base of the trp terminator hairpin, respectively. The efficiency of transcriptional readthrough (%R) was calculated as a fraction of extension products (RO+TP) normalized to 100% readthrough in the presence of IPTG. The results are the mean from three independent experiments ($P < 0.05$).

is proportional to the promoter strength (*5*); hence, it works particularly well at highly expressed genes, such as ribosomal and other stable RNA genes. The majority of genes, however, have relatively weak promoters, which compromise RNAP cooperation at those operons. The backtracking-prone elongation by RNAP, therefore, provides a means for precise adjustment to the rate of translation by a mechanical coupling with a moving ribosome.

Indeed, we observed a perfect match between translation and transcription rates under various growth conditions, including variations in carbon sources and growth-phase transition (Table 1 and figs. S5 to S7). In the stationary phase, transcription and translation rates decelerate synchronously in "wild type" (MG1655) or "slow ribosome" (CH184) cells (figs. S6 and S7 and Table 1). Moreover, Sm accelerated both transcription and translation in the stationary growing CH184 to the levels observed in stationary growing MG1655 (fig. S7 and Table 1). Thus, the transcription elongation rate remains under tight translational control throughout bacterial growth.

In summary, the moving ribosome directly controls the rate of transcription by preventing RNAP from spontaneous backtracking. Because of such cooperation, the rate of transcription is determined by codon usage and nutrient availability sensed by the ribosome. As a result, there is a precise adjustment of transcriptional yield to translational needs under various growth conditions. Macromolecule trafficking and cooperation (fig. S4) is thus the fundamental mechanism of bacterial gene regulation and adaptation to environmental changes.

References and Notes

1. S. Adhya, M. Gottesman, *Annu. Rev. Biochem.* **47**, 967 (1978).
2. J. P. Richardson, *Cell* **64**, 1047 (1991).
3. C. Yanofsky, *Nature* **289**, 751 (1981).
4. Materials and methods are available as supporting material on *Science* Online.
5. V. Epshtein, E. Nudler, *Science* **300**, 801 (2003).
6. U. Vogel, K. F. Jensen, *J. Bacteriol.* **176**, 2807 (1994).
7. K. Bohman, T. Ruusala, P. C. Jelenc, C. G. Kurland, *Mol. Gen. Genet.* **198**, 90 (1984).
8. T. Ruusala, D. Andersson, M. Ehrenberg, C. G. Kurland, *EMBO J.* **3**, 2575 (1984).
9. H. Dong, L. Nilsson, C. G. Kurland, *J. Mol. Biol.* **260**, 649 (1996).
10. Y. Lavner, D. Kotlar, *Gene* **345**, 127 (2005).
11. J. Elf, D. Nilsson, T. Tenson, M. Ehrenberg, *Science* **300**, 1718 (2003).
12. R. Jansen, H. J. Bussemaker, M. Gerstein, *Nucleic Acids Res.* **31**, 2242 (2003).
13. E. Angov, C. J. Hillier, R. L. Kincaid, J. A. Lyon, C. Herman, *PLoS ONE* **3**, e2189 (2008).
14. G. Zhang, Z. Ignatova, A. Idnurm, *PLoS ONE* **4**, e5036 (2009).
15. V. Epshtein, F. Toulmé, A. R. Rahmouni, S. Borukhov, E. Nudler, *EMBO J.* **22**, 4719 (2003).
16. E. Nudler, A. Mustaev, E. Lukhtanov, A. Goldfarb, *Cell* **89**, 33 (1997).
17. N. Komissarova, M. Kashlev, *J. Biol. Chem.* **272**, 15329 (1997).
18. V. Ramakrishnan, *Cell* **108**, 557 (2002).
19. T. A. Steitz, *Nat. Rev. Mol. Cell Biol.* **9**, 242 (2008).
20. G. Bar-Nahum *et al.*, *Cell* **120**, 183 (2005).
21. E. Nudler, *Annu. Rev. Biochem.* **78**, 335 (2009).
22. V. Svetlov, G. A. Belogurov, E. Shabrova, D. G. Vassylyev, I. Artsimovitch, *Nucleic Acids Res.* **35**, 5694 (2007).
23. In addition to preventing backtracking-type pauses, the ribosome can also suppress pausing induced by RNA secondary structures. However, the hairpin-mediated pauses are rare compared with ubiquitous backtracking-type pauses (*25*). They have been detected only within the leader sequences of a few metabolic genes (*3*, *26*) and require specific sequences upstream and downstream of the pause hairpin (*27*). Usually, hairpins do not induce pausing. For example, strong termination hairpins do not pause RNAP (*28*) (fig. S8). Instead, it is a poly-T stretch of the terminator that induces backtracking-type pauses at the site of termination (*28*). Also, factors that suppress RNAP backtracking (e.g., NusG and RfaH) accelerate the overall elongation rate (*20*, *22*)

(fig. S8). Therefore, it is unlikely that random secondary structures affect the overall elongation rate to the same extent as ubiquitous backtracking-type pauses in vivo.
24. H. Saeki, J. Q. Svejstrup, *Mol. Cell* **35**, 191 (2009).
25. M. Depken, E. A. Galburt, S. W. Grill, *Biophys. J.* **96**, 2189 (2009).
26. T. M. Henkin, C. Yanofsky, *Bioessays* **24**, 700 (2002).
27. C. L. Chan, R. Landick, *J. Mol. Biol.* **233**, 25 (1993).
28. I. Gusarov, E. Nudler, *Mol. Cell* **3**, 495 (1999).
29. S. Varenne, J. Buc, R. Lloubes, C. Lazdunski, *J. Mol. Biol.* **180**, 549 (1984).
30. We thank D. Hughes for the CH184 (SmP) strain. This work was supported by grants from the NIH and Dynasty Foundation (E.N.).

Supporting Online Material

www.sciencemag.org/cgi/content/full/328/5977/504/DC1
Materials and Methods
Figs. S1 to S8
References

19 November 2009; accepted 19 February 2010
10.1126/science.1184939